

A Two Competing Substrates Michaelis–Menten Kinetics Scheme for the Analysis of In Vitro Starch Digestograms

Monica Meraz, Jose Alvarez-Ramirez, E. Jaime Vernon-Carter, Isabel Reyes, Carmen Hernandez-Jaimes,* and Filiberto Martinez-Martinez

Progress curves of enzymatic hydrolysis are commonly used for gaining insights on the structure and functionality of native and modified starch. Commonly, heuristic models (e.g., first-order kinetics) are used to fit the experimental data. Models derived from kinetics schemes provide valuable insights on the digestibility properties of starch. In this work, a two competing substrates Michaelis–Menten scheme with enzyme inhibition by-products is used for developing a structured model for enzymatic hydrolysis of starch dispersions. The resulting nonlinear model can provide estimates of the hydrolysis dynamics of rapidly and slowly digested starch fractions. The estimation of parameters is carried out by the numerical solution of a least-squares problem, and illustrated with the hydrolysis by α -amylase of gelatinized corn starch dispersions.

1. Introduction

Studies of in vitro starch digestion by pancreatic α -amylase of starchy foods and starches obtained from different botanical sources are commonly conducted. The in vitro enzymatic hydrolysis tests provide valuable information about starch structure and functionality. The rate at which starch is digested is an important parameter for assessing glucose production which has bearing on human health. The issue is of particular importance in the prevention of life-style related conditions, such as metabolic syndrome and cardiovascular diseases.^[1]

In principle, information on digestibility rates and starch fractions can be extracted from hydrolysis kinetics data obtained from in vitro tests. Mathematical modeling permits predictions

of the hydrolysis behavior under given process conditions. Specifically, a common problem is the description of the experimental data by simple kinetics models while obtaining valuable information of the starch digestibility and potential mechanisms involved in the transformation of starch into simple saccharides. Some attempts in this line have been undertaken in the recent two decades. Goñi et al.^[2] considered that the enzymatic starch hydrolysis followed a first-order kinetics with limiting (i.e., equilibrium) concentration. The model can be written in log–log form as follows: $\ln [(S_\infty - S(t))/S_\infty] = -k_H t$. The concentration at the end of the reaction S_∞ and the rate constant k_H can be obtained by

least-square linear fitting of the progress curve. This model has been extensively used for a large diversity of experimental conditions. However, the first-order kinetics approach can only provide limited performance in many experimental cases. In particular, Butterworth et al.^[3] showed that the enzymatic hydrolysis kinetics can exhibit multi-scale behavior, an effect that the single-exponential model by Goñi et al.^[2] is unable to capture. The analysis of experimental results based on the log-of-slope (LOS) method showed that starch hydrolysis exhibits dynamics at different timescales, a feature that was interpreted as the existence of starch fractions with different digestibility properties.^[4]


Michaelis–Menten models have been also used for describing starch enzymatic hydrolysis. Åkerberg et al.^[5] used Michaelis–Menten models for describing the enzymatic saccharification of wheat starch. Amato et al.^[6] used a simple Michaelis–Menten model with enzyme inactivation for describing enzymatic amylolysis. Similarly, Dona et al.^[7] used single Michaelis–Menten kinetics for analyzing two stages of digestion, which were related to rapidly and slowly digestible starch fractions. The reader is referred to the review by Dona et al.^[8] for a detailed discussion on structured and non-structured models used for the description of kinetics data obtained from in vitro and in vivo tests. In many cases, the kinetics models are based on heuristic extensions of the single-substrate Michaelis–Menten model.

In this work, a two competing substrates Michaelis–Menten scheme including enzyme inhibition by-products was used for developing a structured model for enzymatic hydrolysis of starch. In contrast to reported models, the proposed model was obtained from the application of the principle of mass action. The estimation of the parameters of the resulting nonlinear model was carried out by the numerical solution of a least-squares problem.

Dr. M. Meraz
Departamento de Biotecnología
Universidad Autónoma Metropolitana-Iztapalapa
Apartado Postal 55-534, CDMX, Iztapalapa 09340, México

Dr. J. Alvarez-Ramirez, Dr. E. J. Vernon-Carter, Dr. F. Martinez-Martinez
Departamento de Ingeniería de Procesos e Hidráulica
Universidad Autónoma Metropolitana-Iztapalapa
Apartado Postal 55-534, CDMX Iztapalapa 09340, México

Dr. I. Reyes, Dr. C. Hernandez-Jaimes
Facultad de Ciencias
Universidad Autónoma del Estado de México
Campus El Cerrillo Toluca 50200, México
E-mail: carmenhernandezjaimes@xanum.uam.mx

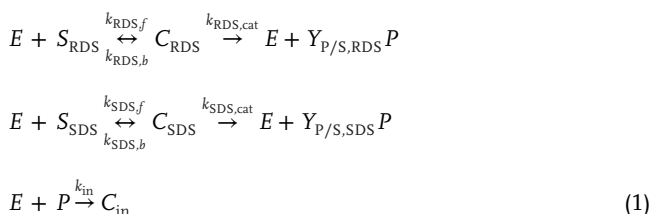
 The ORCID identification number(s) for the author(s) of this article can be found under <https://doi.org/10.1002/star.201900170>

DOI: 10.1002/star.201900170

2. Results and Discussion

2.1. Two Competing Substrates Michaelis–Menten Kinetics Scheme

An approach for the description of the enzymatic hydrolysis of starch is described below. The development of a structured model for starch hydrolysis was made on the basis of a Michaelis–Menten kinetics scheme. Englyst et al.^[9] assumed that starch can be described by three fractions; namely, rapidly digestible starch (RDS), slowly digestible starch (SDS), and resistant starch (RS) fractions. On the other hand, Hill et al.^[10] showed that hydrolysis products (e.g., glucose) inhibit the activity of α -amylase. Enzyme inhibition was corroborated by Aspar and Özbek^[11] in the context of hydrolysis of corn starch dispersions. The mechanisms involved in enzyme inhibition are still unclear. A commonly used approach considers that inhibition is via the formation of inhibitor-enzyme complexes, which enable enzyme to interact with substrates.^[12,13] In the spirit of such results, the following scheme for starch hydrolysis can be proposed



Here, S_{RDS} and S_{SDS} denote, respectively, rapidly and slowly digestible starch fractions, P denotes the hydrolysis products, C_{RDS} and C_{SDS} are enzyme-substrate complexes, and C_{in} is the inhibitor-enzyme complex. On the other hand, k_f , k_b , k_{cat} , and k_{in} represent the forward, backward, catalytic, and inhibition rate constants, and $Y_{\text{P/S,RDS}}$ and $Y_{\text{P/S,SDS}}$ are the respective factor conversions from starch to products. The first two kinetics steps correspond to the degradation of RDS and SDS fractions within a traditional Michaelis–Menten kinetics scheme. The third step describes the inhibition of hydrolysis enzymes by the effect of products. Basically, the kinetics scheme (1) describes a reaction system where the degradation of the SDS fraction appears delayed relative to the degradation of the RDS fraction. Under a sufficient separation of hydrolysis timescales, the SDS fraction would take place after the degradation of the RDS fraction. In the following, the differential equations related to the kinetics scheme (1) will be derived.

The application of the principle of mass action to the kinetics scheme (1) gives the following set of differential equations:

$$\begin{aligned}
 \frac{dS_{\text{RDS}}}{dt} &= k_{\text{RDS},b} C_{\text{RDS}} - k_{\text{RDS},f} E S_{\text{RDS}} \\
 \frac{dS_{\text{SDS}}}{dt} &= k_{\text{SDS},b} C_{\text{SDS}} - k_{\text{SDS},f} E S_{\text{SDS}} \\
 \frac{dE}{dt} &= (k_{\text{RDS},b} + k_{\text{RDS},\text{cat}}) C_{\text{RDS}} - k_{\text{RDS},f} E S_{\text{RDS}} \\
 &\quad + (k_{\text{SDS},b} + k_{\text{SDS},\text{cat}}) C_{\text{SDS}} - k_{\text{SDS},f} E S_{\text{SDS}} - k_{\text{in}} E P
 \end{aligned}$$

$$\begin{aligned}
 \frac{dC_{\text{RDS}}}{dt} &= k_{\text{RDS},f} E S_{\text{RDS}} - (k_{\text{RDS},b} + k_{\text{RDS},\text{cat}}) C_{\text{RDS}} \\
 \frac{dC_{\text{SDS}}}{dt} &= k_{\text{SDS},f} E S_{\text{SDS}} - (k_{\text{SDS},b} + k_{\text{SDS},\text{cat}}) C_{\text{SDS}} \\
 \frac{dP}{dt} &= Y_{\text{P/S,RDS}} k_{\text{RDS},\text{cat}} C_{\text{RDS}} + Y_{\text{P/S,SDS}} k_{\text{SDS},\text{cat}} C_{\text{SDS}} - k_{\text{in}} E P \quad (2)
 \end{aligned}$$

The initial conditions for this set of differential equations are $S_{\text{RDS},0}$ and $S_{\text{SDS},0}$ for RDS and SDS starch, respectively, and E_0 for the amylolytic enzymes. The initial conditions must satisfy the following constraints:

$$S_{\text{RDS},0} + S_{\text{SDS},0} + S_{\text{RS},0} = S_0 \quad (3)$$

where $S_{\text{RS},0}$ denotes the concentration of resistant starch. It should be noted that resistant starch is not affected by enzymatic activity, such that the resistant starch concentration is invariant in the hydrolysis time course; that is, $S_{\text{RS}}(t) = S_{\text{RS},0}$, for all $t > 0$. Zero initial complex concentrations, $C_{\text{RDS},0} = 0$ and $C_{\text{SDS},0} = 0$, are assumed. The mass balance given by Equation (2) is not mutually independent. In fact, the enzyme conservation relationship should be satisfied.

$$C_{\text{RDS}} + C_{\text{SDS}} + C_{\text{in}} + E = E_0 \quad (4)$$

The set of differential equations (2) contains chemical species that are not available for measurements (e.g., complexes). In this regard, a procedure for removing the dynamics of intermediate complexes is required. In fact, the reduction of the order of the system given by equations (2) was made through the elimination of the differential equations governing the intermediate complexes C_{RDS} and C_{SDS} . The traditional derivation of the Michaelis–Menten equation relies on the so-called quasi-steady-state assumption (QSSA), which considers that the concentration of the intermediate complexes hardly changes on the timescale of product. In the case of the system (2), the QSSA implies that $dC_{\text{RDS}}/dt \approx 0$ and $dC_{\text{SDS}}/dt \approx 0$ hold simultaneously. This means that the following equalities are satisfied.

$$\begin{aligned}
 k_{\text{RDS},f} E S_{\text{RDS}} - (k_{\text{RDS},b} + k_{\text{RDS},\text{cat}}) C_{\text{RDS}} &= 0 \\
 k_{\text{SDS},f} E S_{\text{SDS}} - (k_{\text{SDS},b} + k_{\text{SDS},\text{cat}}) C_{\text{SDS}} &= 0
 \end{aligned} \quad (5)$$

Equivalently,

$$\begin{aligned}
 C_{\text{RDS}} &= K_{\text{RDS,QSS}} E S_{\text{RDS}} \\
 C_{\text{SDS}} &= K_{\text{SDS,QSS}} E S_{\text{SDS}}
 \end{aligned} \quad (6)$$

where

$$\begin{aligned}
 K_{\text{RDS,QSS}} &= \frac{k_{\text{RDS},f}}{k_{\text{RDS},b} + k_{\text{RDS},\text{cat}}} \\
 K_{\text{SDS,QSS}} &= \frac{k_{\text{SDS},f}}{k_{\text{SDS},b} + k_{\text{SDS},\text{cat}}}
 \end{aligned} \quad (7)$$

Then, the system of differential equations given by Equation (2) can be reduced to the following one.

$$\begin{aligned}\frac{dS_{RDS}}{dt} &= (k_{RDS,b}K_{RDS,QSS} - k_{RDS,f}) ES_{RDS} \\ \frac{dS_{SDS}}{dt} &= (k_{SDS,b}K_{SDS,QSS} - k_{SDS,f}) ES_{SDS} \\ \frac{dE}{dt} &= -k_{in}EP \\ \frac{dP}{dt} &= Y_{P/S,RDS}k_{RDS,cat}K_{RDS,QSS}ES_{RDS} \\ &\quad + Y_{P/S,SDS}k_{SDS,cat}K_{SDS,QSS}ES_{SDS} - k_{in}EP\end{aligned}\quad (8)$$

The substrates $S_{RDS}(t)$ and $S_{SDS}(t)$ should decay with time. In this way, the parametric constraint

$$\begin{aligned}k_{RDS,b}K_{RDS,QSS} - k_{RDS,f} &< 0 \\ k_{SDS,b}K_{SDS,QSS} - k_{SDS,f} &< 0\end{aligned}\quad (9)$$

should be satisfied. From (7), these inequalities are equivalent to the following ones.

$$\begin{aligned}\frac{k_{RDS,b}}{k_{RDS,b} + k_{RDS,cat}} &< 1 \\ \frac{k_{SDS,b}}{k_{SDS,b} + k_{SDS,cat}} &< 1\end{aligned}\quad (10)$$

This implies that the inequalities (9) are satisfied for all values of the kinetics parameters.

2.2. Two Competing Substrates Michaelis–Menten without Enzyme Inhibition

The model (5) was derived from a Michaelis–Menten kinetics scheme. The consistency of this model was checked by showing that it is reduced to a form of the traditional Michaelis–Menten equation for two substrates. To this end, consider Equation (8) with $k_{in} = 0$. In this way, Equation (8) are reduced to the following system.

$$\begin{aligned}\frac{dS_{RDS}}{dt} &= (k_{RDS,b}K_{RDS,QSS} - k_{RDS,f}) ES_{RDS} \\ \frac{dS_{SDS}}{dt} &= (k_{SDS,b}K_{SDS,QSS} - k_{SDS,f}) ES_{SDS} \\ \frac{dP}{dt} &= Y_{P/S,RDS}k_{RDS,cat}K_{RDS,QSS}ES_{RDS} \\ &\quad + Y_{P/S,SDS}k_{SDS,cat}K_{SDS,QSS}ES_{SDS}\end{aligned}\quad (11)$$

In the same way, by recalling that $C_{in} = 0$ the enzyme conservation (4) gives

$$E = E_0 - C_{RDS} - C_{SDS}\quad (12)$$

The combination of this expression with Equation (6) leads to the following expressions.

$$\begin{aligned}(1 + K_{RDS,QSS}S_{RDS})C_{RDS} + K_{RDS,QSS}S_{RDS}C_{SDS} &= K_{RDS,QSS}E_0S_{RDS} \\ K_{SDS,QSS}S_{SDS}C_{RDS} + (1 + K_{SDS,QSS}S_{SDS})C_{SDS} &= K_{SDS,QSS}E_0S_{SDS}\end{aligned}\quad (13)$$

These two linear equations can be solved for the complexes C_{RDS} and C_{SDS} to give

$$\begin{aligned}C_{RDS} &= \frac{K_{RDS,QSS}E_0S_{RDS}}{1 + K_{RDS,QSS}S_{RDS} + K_{SDS,QSS}S_{SDS}} \\ C_{SDS} &= \frac{K_{SDS,QSS}E_0S_{SDS}}{1 + K_{RDS,QSS}S_{RDS} + K_{SDS,QSS}S_{SDS}}\end{aligned}\quad (14)$$

It is noted that $1 + K_{RDS,QSS}S_{RDS} + K_{SDS,QSS}S_{SDS} > 0$, which guarantees the validity of the above solutions. In this way, the enzyme concentration defined by Equation (12) is given by

$$E = \frac{E_0}{1 + K_{RDS,QSS}S_{RDS} + K_{SDS,QSS}S_{SDS}}\quad (15)$$

After substitution of Equation (15) in Equation (11), one obtains

$$\begin{aligned}\frac{dS_{RDS}}{dt} &= \frac{(k_{RDS,b}K_{RDS,QSS} - k_{RDS,f})E_0S_{RDS}}{1 + K_{RDS,QSS}S_{RDS} + K_{SDS,QSS}S_{SDS}} \\ \frac{dS_{SDS}}{dt} &= \frac{(k_{SDS,b}K_{SDS,QSS} - k_{SDS,f})E_0S_{SDS}}{1 + K_{RDS,QSS}S_{RDS} + K_{SDS,QSS}S_{SDS}} \\ \frac{dP}{dt} &= \frac{Y_{P/S,RDS}k_{RDS,cat}K_{RDS,QSS}E_0S_{RDS} + Y_{P/S,SDS}k_{SDS,cat}K_{SDS,QSS}E_0S_{SDS}}{1 + K_{RDS,QSS}S_{RDS} + K_{SDS,QSS}S_{SDS}}\end{aligned}\quad (16)$$

For a single substrate, say S , the above system is reduced to the following differential equations.

$$\begin{aligned}\frac{dS}{dt} &= \frac{(k_bK_{QSS} - k_f)E_0S}{1 + K_{QSS}S} \\ \frac{dP}{dt} &= \frac{Y_{P/S}k_{cat}K_{QSS}E_0S}{1 + K_{QSS}S}\end{aligned}\quad (17)$$

which is the classical Michaelis–Menten equation with $K_{MM} = K_{QSS}^{-1}$ being the Michaelis–Menten constant. In this way, $K_{MM,RDS} = K_{QSS,RDS}^{-1}$ and $K_{MM,SDS} = K_{QSS,SDS}^{-1}$ correspond to the Michaelis–Menten constants for RDS and SDS fractions. It is concluded that Equation (16) are the generalization of the traditional Michaelis–Menten equation for two substrates. Since the system (16) is a particular case of Equation (8), in turn this system can be seen as an extension of the traditional Michaelis–Menten equation for two substrates and enzyme inhibition by-products.

2.3. Simplification of Model (8) for Digestogram Analysis

In principle, the model given by Equation (8) can be used for the analysis of starch digestograms. This model involves both substrate and product dynamics. In practice, digestograms are obtained by subjecting starch dispersions to the action of a blend of amylolytic enzymes, mainly amylases and estimating the progress of the starch hydrolytic degradation. The most common approach for in vitro digestibility tests consists of measuring the generation of products in the form of total glucose. In turn, the amount of products is linked to the progress of starch hydrolysis via a simple yield relationship of the form

$$S_0 - S(t) = 0.9(P(t) - P_0) \quad (18)$$

where 0.9 is the glucose-to-starch factor conversion.^[2] By doing this, digestograms in the starch literature are commonly presented as the progress of either the substrate concentration $S(t)$ or the respective conversion. In terms of the kinetics scheme (1), the expression (18) can be extended as follows.

$$P(t) - P_0 = Y_{P/S,RDS} (S_{RDS,0} - S_{RDS}) + Y_{P/S,SDS} (S_{SDS,0} - S_{SDS}) \quad (19)$$

A further reasonable assumption is that $Y_{P/S,RDS} \approx Y_{P/S,SDS} \equiv Y_{P/S}$, such that the above expression becomes

$$P(t) = P_0 + Y_{P/S} [(S_{RDS,0} + S_{SDS,0}) - (S_{RDS}(t) + S_{SDS}(t))] \quad (20)$$

In a simplified setting, the use of Equation (20) allows the further reduction of Equation (8) by discarding of the dynamics of the products; namely

$$\begin{aligned} \frac{dS_{RDS}}{dt} &= (k_{RDS,b}K_{RDS,QSS} - k_{RDS,f}) ES_{RDS} \\ \frac{dS_{SDS}}{dt} &= (k_{SDS,b}K_{SDS,QSS} - k_{SDS,f}) ES_{SDS} \\ \frac{dE}{dt} &= -k_{in}EP \end{aligned} \quad (21)$$

In this case, the time course of the products is computed by means of the relationship (20) with $Y_{P/S} = 1/0.9 \approx 1.11$.^[2] The set of differential equations (21) together with the algebraic relationship (20) describe the time course of the digestible starch fractions S_{RDS} and S_{SDS} , and the available enzyme $E(t)$.

2.4. Estimation of Parameters

The model (21) is the most affordable for the analysis of hydrolysis time courses obtained from in vitro digestibility tests. The idea is to use this model for estimating the digestible fractions contained in a starch sample. In turn, these fractions correspond to the initial conditions $S_{RDS,0}$ and $S_{SDS,0}$, which are not known in advance. Importantly, $S_{RDS,0}$ and $S_{SDS,0}$ can be seen as parameters that should be estimated from experimental digestograms, and the estimation should include the kinetics constants contained in the system given by Equation (21).

To address the estimation of parameters, it is convenient to rewrite the system (21) as follows.

$$\begin{aligned} \frac{dS_{RDS}}{dt} &= -k_{H,RDS}ES_{RDS} \\ \frac{dS_{SDS}}{dt} &= -k_{H,SDS}ES_{SDS} \\ \frac{dE}{dt} &= -k_{in}E (P_0 + Y_{P/S} [(S_{RDS,0} + S_{SDS,0}) - (S_{RDS} + S_{SDS})]) \end{aligned} \quad (22)$$

Here, after using Equation (7), one has that

$$\begin{aligned} k_{H,RDS} &= k_{RDS,f} \frac{k_{RDS,cat}}{k_{RDS,b} + k_{RDS,cat}} \\ k_{H,SDS} &= k_{SDS,f} \frac{k_{SDS,cat}}{k_{SDS,b} + k_{SDS,cat}} \end{aligned} \quad (23)$$

are defined as the corresponding hydrolysis kinetics constants. The two competing substrates model (22) depends on five unknown parameters; namely

$$\Pi = \{k_{H,RDS}, k_{H,SDS}, k_{in}, S_{RDS,0}, S_{SDS,0}\} \quad (24)$$

In particular, the initial conditions $S_{RDS,0}$ and $S_{SDS,0}$ are taken as the RDS and SDS contents in the starch sample. In principle, this set of parameters can be estimated from a given time course of the substrate consumption. For a set of N pointwise experimental measurements in the time course of the starch depletion time course, say $\{S(t_1)_{exp}, S(t_2)_{exp}, \dots, S(t_N)_{exp}\}$ with t_1, t_2, \dots, t_N being the measurement times, the estimation of parameters can be carried out with the following steps.

- Step 1.** Set the initial enzyme E_0 , and starch S_0 concentrations.
- Step 2.** Set an initial guess for the parameter set $\Pi = \{k_{H,RDS}, k_{H,SDS}, k_{in}, S_{RDS,0}, S_{SDS,0}\}$. All parameters must be nonnegative. The constraint $S_{RDS,0} + S_{SDS,0} + S_{RS} = S_0$ should be satisfied. In this case, S_{RS} is the starch that has the ability to survive prolonged (i.e., very long times) incubation with α -amylase and other amylolytic enzymes.^[14] The determination of S_{RS} can be carried out by the method described by Goñi et al.^[15]
- Step 3.** Solve iteratively a nonlinear least-squares problem for the objective function

$$\min_{\Pi} \frac{1}{N} \sum_{j=1}^N \left(\frac{S(t_j)_{exp} - S(t_j)_{est}}{S(t_j)_{est}} \right)^2 \quad (25)$$

where the estimated concentrations $\{S(t_1)_{est}, S(t_2)_{est}, \dots, S(t_N)_{est}\}$ are obtained from the numerical integration of the Michaelis–Menten model given by the system (22). For each iteration, check the fulfillment of the constraint $S_{RDS,0} + S_{SDS,0} + S_{RS} = S_0$.

- Step 4.** From the final set of estimated parameters, the RDS and SDS fractions are given by $S_{RDS,0}$ and $S_{SDS,0}$, respectively.

The computational complexity of solving the above problem of parameters estimation is higher than the problem involved with

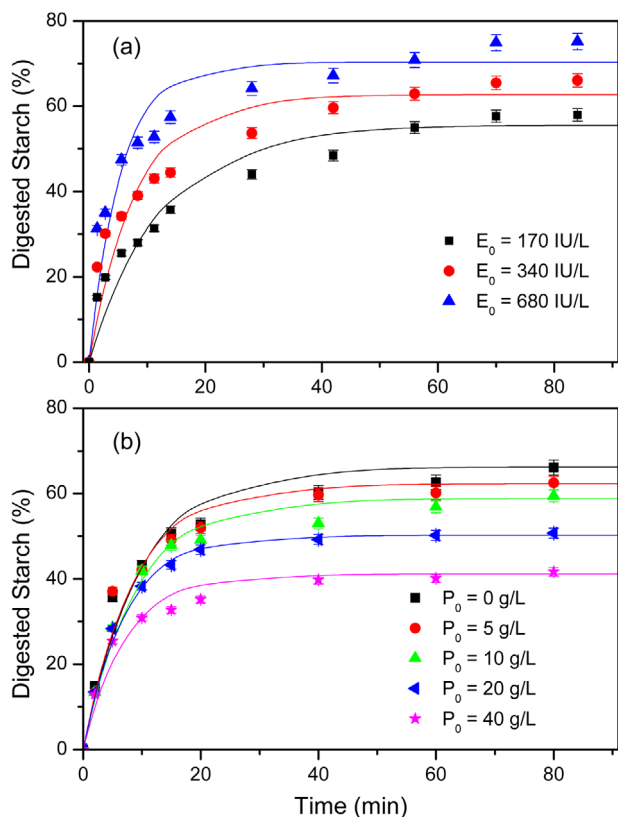


Figure 1. Progress curve of starch hydrolysis for a) different α -amylase concentrations, and b) different initial glucose concentrations. The continuous lines denote the best least-squares fitting to the first-order exponential model of Equation (26). Error bars in experimental data correspond to standard deviations from the mean for three replicates.

the simple exponential function model by Goñi et al.^[2]. However, the two competing substrates Michaelis–Menten (21) provides more detailed information (e.g., enzyme inhibition) on the kinetics of the starch enzymatic hydrolysis. It is in general expected that the more detailed kinetics modeling is accompanied by the solution of problems with increased computational complexity.

2.5. Example

A simple example will be used to illustrate the ability of the derived Michaelis–Menten model to describe progress curves obtained from amyolytic reactions of starch dispersions. It should be pointed out that, rather than providing a detailed description of the physicochemical mechanisms involved in the starch hydrolysis, the focus will be on the fitting procedure and the physical consistency of the estimated parameters. The moisture content in the native starch is about 14.5%, such that initial substrate concentration was about $S_0 = 45.5 \text{ g L}^{-1}$. Besides, the concentration of the RS component was about 2.5% as determined by the method of Goñi et al.^[15] **Figure 1a** presents the hydrolysis kinetics for three different values of the α -amylase concentration. It is apparent that the hydrolysis reaction is slowed as the enzyme concentration was reduced. Besides, the maximum value of the

Table 1. Kinetics parameters corresponding to the first-order model (Equation (26)) of the starch hydrolysis for three different initial enzyme concentrations (upper panel), and five different glucose concentrations (lower panel).

E_0 [IU L ⁻¹]	$k_H \times 10^1$ [1 min ⁻¹]	x_∞ [%]	Err [%]	Z_{ff}
170	1.22 ± 0.04 ^a	48.96 ± 1.27 ^c	6.38	1.30
354	2.07 ± 0.05 ^b	54.77 ± 2.31 ^b	5.91	1.30
680	2.73 ± 0.07 ^c	64.11 ± 1.87 ^a	5.08	1.28
P_0 [g L ⁻¹]	$k_H \times 10^1$ [1 min ⁻¹]	x_∞ [%]	Err [%]	Z_{ff}
0	1.27 ± 0.05 ^b	64.55 ± 1.21 ^a	3.82	1.30
5	1.28 ± 0.06 ^b	61.69 ± 1.11 ^b	3.45	0.98
10	1.29 ± 0.05 ^{ab}	57.99 ± 1.06 ^c	2.89	1.30
20	1.36 ± 0.05 ^a	50.05 ± 1.15 ^d	2.88	1.35
40	1.32 ± 0.06 ^a	40.08 ± 1.05 ^e	3.95	1.30

Mean ± standard error, $n = 3$. Means in columns not sharing the same letter are significantly different at $p < 0.05$, according to Tukey's test.

hydrolysis advance was limited by the reduction of the enzyme concentration. This effect suggests that α -amylase was subjected to inhibition by the products of the hydrolysis, an effect that was reported by Hill et al.^[10] and by Aspar and Özbek.^[11] Hydrolysis runs under different glucose concentrations were conducted for corroborating the inhibition of α -amylase, and the results are shown in Figure 1b. Interestingly, the initial addition of glucose reduced the maximum achievable starch hydrolysis, and this effect was more pronounced when the initial glucose concentration was increased. As mentioned above, the mechanisms behind the enzyme inhibition are not clear at all, although it was postulated that the formation of a complex between α -amylase and glucose molecules could be involved.^[10,11] The model given by (22) incorporates this effect and, in principle has the ability of fitting the experimental data in Figure 1.

The first-order exponential model by Goñi et al.^[2] has been widely used for fitting the amyolytic hydrolysis of starch dispersions. In terms of the total substrate concentration, Goñi et al.'s model can be written as follows.

$$S(t) = S_0 \exp(-k_H t) + S_\infty (1 - \exp(-k_H t)) \quad (26)$$

Here, $S(t)$ is the total substrate concentration, S_∞ is the limiting concentration achieved for long times, and k_H is the hydrolysis rate constant. Although Equation (26) is simple, it provides an estimation of the rate at which starch is hydrolyzed by the action of amyolytic enzymes. The continuous lines in Figure 1 depict the least-squares fitting of experimental data. The fitting is acceptable for short and long hydrolysis times as the numerical fitting forced the initial $S(0) = S_0$ and equilibrium $S(t) \rightarrow S_\infty$ constraints. However, important deviations were observed for medium-term times. The fitting error is defined as

$$\text{Err} = \frac{1}{N} \sum_{j=1}^N \left(\frac{S_{\text{exp}}(t_j) - S_{\text{est}}(t_j)}{S_{\text{exp}}(t_j)} \right)^2 \quad (27)$$

Also, $x_\infty = (S_0 - S_\infty)/S_0$ denotes the limiting starch conversion. **Table 1** shows the estimates of the model parameters and the fitting error. The values of hydrolysis rate constant increased

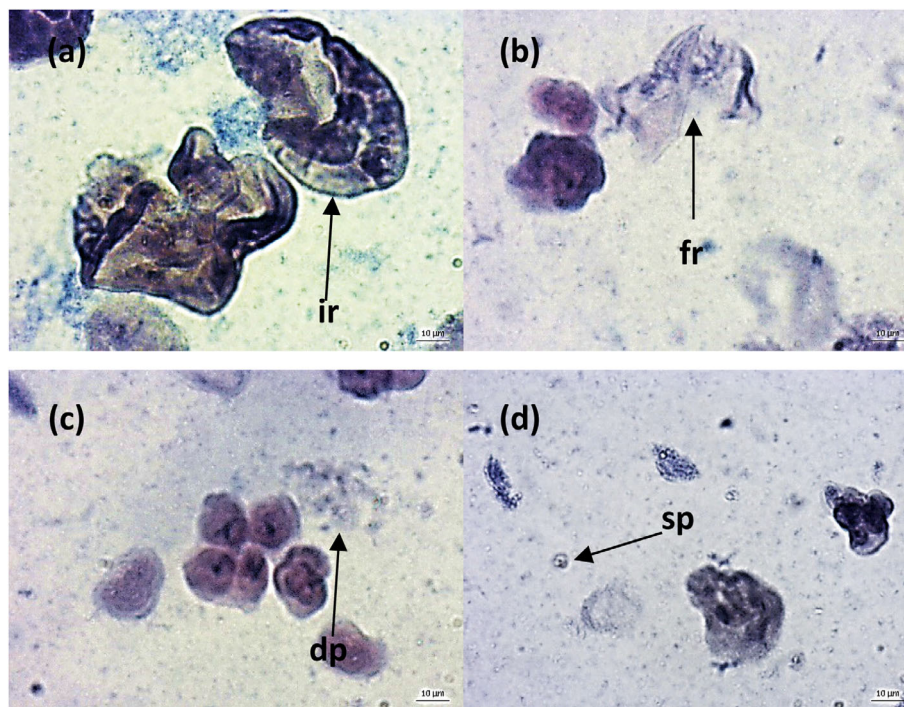


Figure 2. Light microscopy images of the starch dispersion at four different hydrolysis times. a) 0 min, b) 20 min, c) 40 min, and d) 60 min. ir, immiscible remnants; fr, fractured remnant; dp, digested particle; sp, small particles.

with the enzyme concentration, reflecting the fact that the reaction rate is faster for higher concentrations of enzymes. The opposite effect was observed for the initial glucose concentration where the hydrolysis rate constant showed a weak reduction with the increase of initial glucose concentration. The fitting errors are relatively high, with values ranging from 3% to 6%. These values are linked to important fitting deviations observed for medium times, at the crossover between the initial fast hydrolysis and the hydrolysis slowing phase for long times. For all cases, the estimate of the standard normal deviates is unacceptably high as the set critical value is 0.976 ($p < 0.05$). In fact, the values of Z_{ij} are higher than 0.976, indicating that the residuals are not randomly distributed about the fitted curve.

In general terms, the first-order exponential model provides unacceptable description of the experimental data. The slower starch hydrolysis compared to the prediction made by the first-order exponential model Equation (26) suggests the presence of a starch fraction that is digested at smaller rates, which motivates the application of a more involved model. Images in **Figure 2** illustrate the evolution of the starch hydrolysis (340 IU L^{-1} , $P_0 = 0.0 \text{ g L}^{-1}$) for four different times; namely, a) 0, b) 20, c) 40, and d) 60 min. The arrow in Figure 2a indicates the insoluble remnants (tagged as “ir”), also known as ghosts, which remained after gelatinization. These structures are likely to show reduced digestion relative to starch chains leached out during the gelatinization process. After 20 min of exposition to amylolytic enzymes, the insoluble remnants exhibited some fragmented remnants (tagged as “fr”), as indicated by the arrow in Figure 2b. For longer hydrolysis times, the otherwise solid structures were completely fragmented, giving rise to digested particles (tagged as “dp” in Figure 2c) and many small particles (tagged as “sp”

in Figure 2d) dispersed in the continuous phase. In turn, the continuous phase is composed mainly of amylose chains. After gelatinization, a dispersed phase made up of insoluble remnants that are composed of amylopectin chains crosslinked by small fractions of lipids and proteins remains.^[16] These insoluble remnants, also known as ghosts, are gradually hydrolyzed, although Figure 2 suggests that the hydrolysis rate is relatively slower compared to that of soluble chains in the continuous phase. Images in Figure 2 suggest that the hydrolysis process is carried out at different timescales. In line with findings by LOS method,^[3] the mono-scale Goñi et al.’s model (26) can be extended to a two-scale equation to account for multi-scale hydrolysis reactions. In this way, a straightforward two-scale extension of Equation (26) can be written as follows.

$$S(t) = S_{\infty} + a_f \exp(-k_{H,f}t) + a_s \exp(-k_{H,s}t) \quad (28)$$

Here, $k_{H,f}$ and $k_{H,s}$ ($k_{H,f} > k_{H,s}$) are rate constants for fast and slow timescales, respectively. The parameters a_f and a_s are pre-exponential factors satisfying $a_f + a_s = S_0 - S_{\infty}$. **Figure 3** presents the least-squares fittings by Equation (28). Note that the fitting curve provides a better description of the experimental data over the whole time range. This suggests that the starch hydrolysis by amylolytic enzyme is carried out under a multi-scale kinetics process. **Table 2** describes the estimated parameters and the fitting error. For all cases, the estimation error is smaller than 1%, showing that the second-order exponential model (28) provided an enhanced description of the experimental data as compared to the traditional Goñi et al.’s Equation (26). Interestingly, the fast hydrolysis rate constant $k_{H,f}$ is about tenfold the slow hydrolysis rate constant $k_{H,s}$, which indicates a clear separation of the

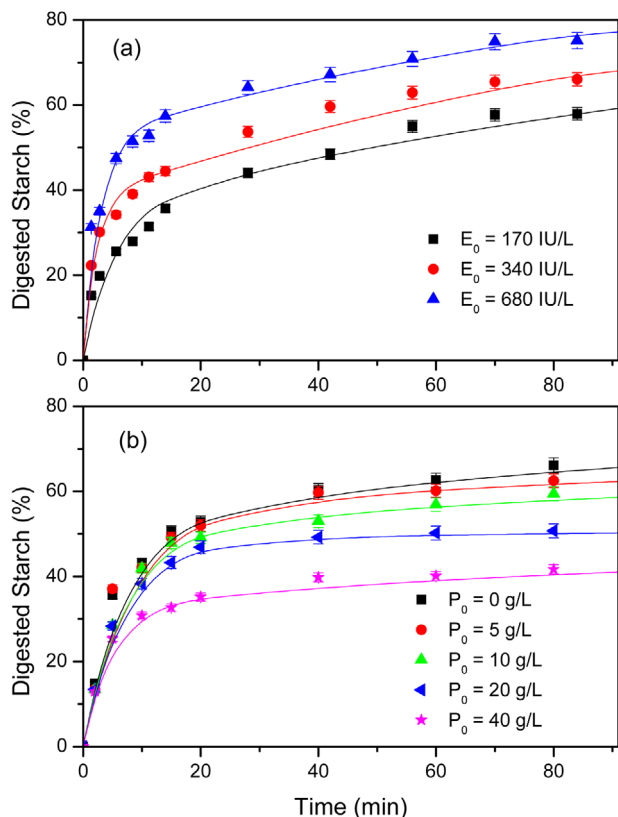


Figure 3. Progress curve of starch hydrolysis for different a) α -amylase concentrations and b) different initial glucose concentrations. Error bars in experimental data correspond to standard deviations from the mean for three replicates. The continuous lines denote the best least-squares fitting to the second-order exponential model of Equation (28).

Table 2. Kinetics parameters from the second-order exponential model Equation (28) of the starch hydrolysis for three different initial enzyme concentrations (upper panel), and five different initial glucose concentration (lower panel).

E_0 [IU L ⁻¹]	$k_{H,f} \times 10^1$ [1 min ⁻¹]	$k_{H,S} \times 10^2$ [1 min ⁻¹]	Err [%]	Z_{ff}
170	1.18 ± 0.09 ^c	1.07 ± 0.13 ^a	0.52	0.18
354	1.65 ± 0.11 ^b	1.12 ± 0.11 ^b	0.64	0.18
680	3.77 ± 0.10 ^a	0.97 ± 0.08 ^c	0.76	0.18
P_0 [g L ⁻¹]	$k_{H,f} \times 10^1$ [1 min ⁻¹]	$k_{H,S} \times 10^2$ [1 min ⁻¹]	Err [%]	Z_{ff}
0	1.45 ± 0.08 ^b	1.12 ± 0.06 ^a	0.51	0.91
5	1.27 ± 0.06 ^{bc}	1.06 ± 0.05 ^a	0.79	0.18
10	1.49 ± 0.07 ^b	1.02 ± 0.06 ^a	0.28	0.26
20	1.47 ± 0.06 ^b	1.06 ± 0.06 ^a	0.19	0.13
40	2.21 ± 0.09 ^a	1.06 ± 0.04 ^a	0.32	0.91

Mean ± standard error, $n = 3$. Means in columns not sharing the same letter are significantly different at $p < 0.05$, according to Tukey's test.

hydrolysis timescales. This feature is in line with recent findings by LOS method,^[3] which showed that the kinetics of the starch hydrolysis exhibits two-scale behavior. The runs tests reflected by Z_{ff} indicates that the residual can be considered randomly distributed, such that the least-fitting can be considered as acceptable ($p < 0.05$).

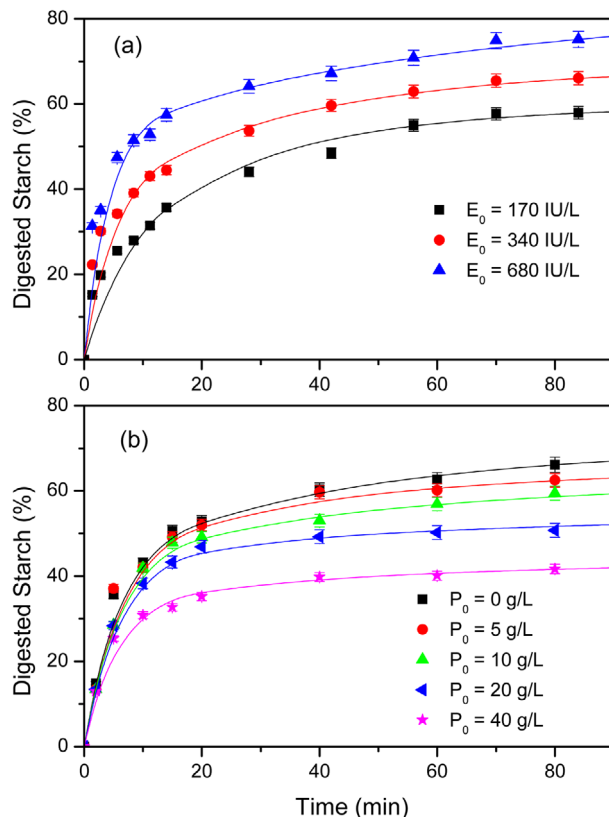


Figure 4. Progress curve of starch hydrolysis for different a) α -amylase concentrations and b) different initial glucose concentrations. Error bars in experimental data correspond to standard deviations from the mean for three replicates. The continuous lines denote the best least-squares fitting to the Michaelis–Menten model Equation (22).

The Michaelis–Menten model given by Equation (22) was also used for describing the experimental data, and the fitting results are presented in **Figures 4** and **5**. The fitting resulting from the model (22) exhibited fitting error values slightly smaller than those obtained with the second-order exponential model (28). In fact, the estimated parameters shown in **Table 3** indicate that the mean error was not higher than 0.5%. The reduced fitting error was obtained thanks to the fact that the model included a description of the enzyme inhibition by hydrolysis products. The runs test also shows that the fitting is acceptable ($p < 0.05$) in terms of the distribution of residuals. The kinetics parameter k_{RDS} is about 20–50 times higher than the kinetics parameter k_{SDS} , indicating a clear scale separation in the enzymatic degradation of the starch fractions RDS and SDS. The model (22) also provides an estimate of the digestible starch fractions. It is noted that relative contents of RDS and SDS depends on the enzyme concentration. In fact, it was found that the RDS fraction increased with the initial enzyme concentration. In contrast, the content of the RDS fraction decreased with the initial glucose concentration, reflecting a faster inhibition of amylolytic enzymes. For $E_0 = 340$ IU L⁻¹ and $P_0 = 0$ g L⁻¹, **Figure 6** presents the estimated kinetics of the fractions RDS and SDS. As estimated by the kinetics parameters, the RDS fraction decayed rapidly, within the first 20 min. Interestingly, the period of 20 min is the time used for estimating the RDS fraction by the Englyst's method.^[9] On the other hand, the

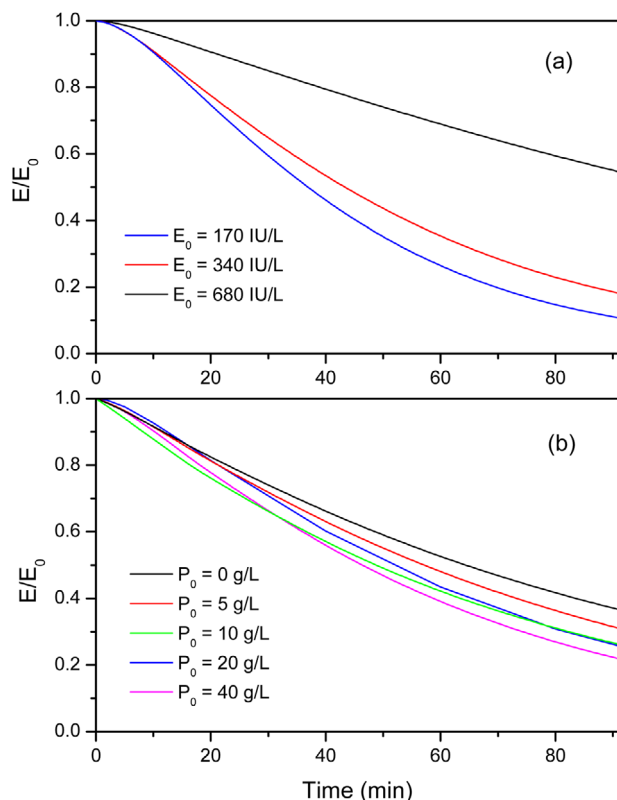


Figure 5. Estimated kinetics of active enzyme obtained from the fitting of Equation (22) to experimental data. (a) Effect of the initial enzyme concentration, and (b) effect of the initial glucose concentration.

SDS fraction exhibited a slow decay, without completed degradation as a consequence of the inhibition of the amylolytic enzymes by-products (i.e., glucose). Usually, the starch fraction remaining after 120 min is considered as resistant starch by the Englyst's method, such that in this case the estimated resistant starch fraction within the first 120 min would be about 32%, which is taken as the addition of the undigested starch fraction and the authentic resistant starch fraction that resist at-large amylolytic hydrolysis.

Table 3. Kinetics parameters from the Michaelis–Menten model Equation (22) of the starch hydrolysis for three different initial enzyme concentrations (upper panel), and five different initial glucose concentration (lower panel).

E_0 [IU L ⁻¹]	$k_{RDS} \times 10^3$ [L IU ⁻¹ min ⁻¹]	$k_{SDS} \times 10^5$ [L IU ⁻¹ min ⁻¹]	$k_{in} \times 10^4$ [L g ⁻¹ min ⁻¹]	RDS [%]	SDS [%]	Err [%]	Z_{ff}
170	1.16 ± 0.10 ^c	2.14 ± 0.11 ^c	1.47 ± 0.06 ^a	16.37 ± 0.71 ^a	81.12 ± 2.69 ^a	0.82	0.13
354	1.96 ± 0.12 ^a	4.72 ± 0.12 ^b	1.24 ± 0.07 ^b	28.28 ± 0.54 ^b	69.21 ± 2.17 ^b	0.93	0.13
680	1.85 ± 0.09 ^{ab}	6.85 ± 0.14 ^a	0.89 ± 0.06 ^c	47.01 ± 0.53 ^a	50.48 ± 1.86 ^c	1.23	0.91
P_0 [g L ⁻¹]	$k_{RDS} \times 10^3$ [L IU ⁻¹ min ⁻¹]	$k_{SDS} \times 10^5$ [L IU ⁻¹ min ⁻¹]	$k_{in} \times 10^4$ [L g ⁻¹ min ⁻¹]	RDS [%]	SDS [%]	Err [%]	Z_{ff}
0	1.21 ± 0.04 ^a	2.25 ± 0.04 ^a	1.43 ± 0.08 ^e	44.93 ± 1.23 ^a	53.06 ± 1.54 ^e	0.82	0.91
5	1.19 ± 0.05 ^{ab}	1.63 ± 0.05 ^b	2.33 ± 0.07 ^d	29.10 ± 1.76 ^b	68.39 ± 1.73 ^d	1.13	0.91
10	1.18 ± 0.07 ^b	1.20 ± 0.04 ^c	3.21 ± 0.07 ^c	25.86 ± 1.98 ^b	72.21 ± 1.36 ^c	0.59	0.91
20	0.98 ± 0.07 ^c	0.52 ± 0.03 ^d	4.27 ± 0.06 ^b	17.34 ± 1.37 ^c	80.15 ± 1.74 ^b	0.33	0.13
40	1.06 ± 0.08 ^c	0.49 ± 0.02 ^d	6.36 ± 0.08 ^a	8.60 ± 0.92 ^d	88.89 ± 1.96 ^a	0.51	0.83

Mean ± standard error, $n = 3$. Means in columns not sharing the same letter are significantly different at $p < 0.05$, according to Tukey's test. RDS: rapidly digestible starch; SDS: slowly digestible starch.

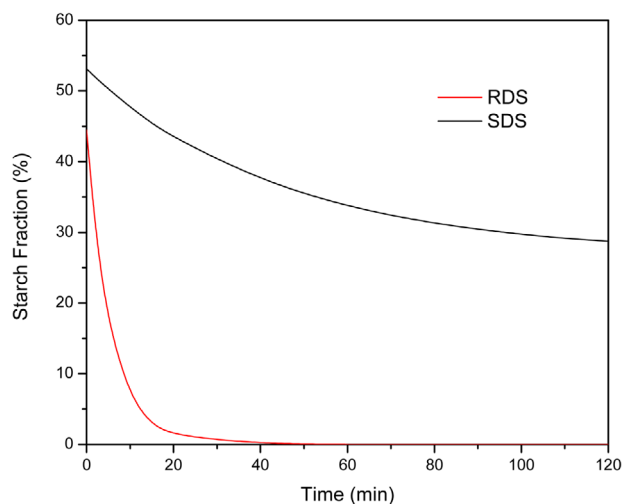


Figure 6. Illustrative example of the kinetics of the RDS and SDS fractions from the Michaelis–Menten model (22). RDS: rapidly digestible starch; SDS: slowly digestible starch.

3. Conclusions

The present work developed a structured model for the enzymatic hydrolysis of starch dispersions. The modeling approach was based on two competing substrates Michaelis–Menten kinetics, in order to account for the rapidly and slowly digestible starch fractions. The scheme includes enzyme inhibition by-products, an effect previously reported by several authors. The resulting model is nonlinear, and requires the numerical solution of a least-squares problem for the estimation of the parameters. Besides, the model provides estimation of the rapidly and slowly digested starch fractions. The model was applied to data obtained from the amylolysis of gelatinized dispersions of corn starch with three different amylose contents, and five different initial glucose concentrations. The model was able to provide improved least-squares fitting than first and second order models currently used for this purpose. Overall, the proposed model provides a suitable framework for the accurate interpretation of experimental (e.g., in vitro) data on enzymatic hydrolysis of starchy systems.

4. Experimental Section

Materials: Native corn starch (CAS number 9005-25-8, amylose content 25.3%, moisture content < 15%, pH 4.8; ash < 0.5%, protein < 0.1%), and α -amylase from porcine pancreas (CAS A3176, pH 5.5–8.0, 51–54 kDa, 300 U mL⁻¹) were purchased from Sigma-Aldrich (St. Louis, MO, USA). All water used in the experiments was deionized.

Enzymatic Hydrolysis: Native corn starch (5.0 g) was dispersed in 100 mL of distilled water and heated (95 °C, 20 min) with continuous mild stirring conditions until complete gelatinization of starch granules was achieved. The dispersions were allowed to cool down to room temperature (\approx 20 °C). The starch dispersions were incubated with porcine pancreatic α -amylase at 37 °C for 120 min, and pH 6.8, in a sealed dialysis bag to avoid ethanol vaporization. The hydrolysis was carried out under two conditions: a) Three different concentrations of porcine α -amylase (63, 126, 256 g L⁻¹ of protein or \approx 170, 340, 680 IU L⁻¹) were used for assessing the effect of the enzyme concentration; b) By fixing the initial enzyme concentration at 126 g L⁻¹ (i.e., 340 IU L⁻¹), and using five different concentrations of glucose (0, 5, 10, 20, and 40 g L⁻¹) for evaluating the potential enzyme inhibition by-products of the hydrolysis. Samples were withdrawn at time intervals up to 120 min and transferred to an ice cold water bath to stop the reaction. The hydrolysis advance was determined measuring the reducing sugar content released at different times by the DNS technique described by Miller,^[17,18] with slight modifications. Briefly, an aliquot (500 μ L) from hydrolytic dispersion was homogenized in a Vortex (Barnstead/ThermoLyne, Dubuque, IA, USA) for 30 s, then the aliquot was centrifuged at 10⁴ rpm for 60 s. Supernatant (200 μ L), deionized water (800 μ L), and DNS reactive (1000 μ L) were gently mixed into an assay tube and immediately was put in a bath of boiling water for 10 min and then cooled in an ice bath during 10 min before reading in a GENESYS 10S UV–Vis spectrophotometer (Thermo Scientific, Waltham, MA) at 540 nm using adequate dilution. Results were reported as maltose equivalents by using a calibrated standard curve. Data were plotted as the degree of hydrolysis versus time. Experiments were done in triplicate.

Optical Microscopy: Optical microscopy was used for illustrating the microstructure of the hydrolyzed starch dispersions. To this end, an optical microscope (Olympus BX45, Olympus Optical Co. Ltd., Tokyo, Japan) was used, and micrographs were captured with an image analyzer system (AxioCamERC5s camera and Zen blue edition software, Carl Zeiss Microscopy GmbH, Göttingen, Germany). Selected micrographs at ocular magnification 10 \times and objective magnification 4 \times are presented.

Data Analysis: The data were expressed as means \pm SD. Statistical analysis of the results were subjected to analysis of variance using the Statgraphics 7 statistical analysis system (Statistical Graphics Corp. Manugistics Inc., Cambridge, MA, USA). When it was pertinent, significant differences ($p < 0.05$) between means were detected with Tukey's test.^[19]

A least-squares fitting by models can follow the trend of the experimental data. However, the fitting residuals can exhibit some correlation patterns, in such a way that the fitting is not acceptable. An important question is whether or not the fitting is acceptable in the sense that residuals are randomly distributed. The distribution of residuals can be analyzed quantitatively by means of the Wald–Wolfowitz runs test.^[20,21] In this approach, a run is a sequence of consecutive points having a residual of the same sign. The number of runs, say R , is computed from the total number of positive (n_p) and negative (n_n) residuals as follows:

$$R = \frac{2n_p n_n}{n_p + n_n} + 1 \quad (29)$$

On the other hand, the variance of the expected number of runs is given by

$$\sigma_R^2 = \frac{2n_p n_n (2n_p n_p - n_p - n_n)}{(n_p + n_n)^2 (n_p + n_n - 1)} \quad (30)$$

A comparison between R and the observed number of runs n_R provides an estimate of the standard normal deviate; namely,

$$Z_{tf} = \frac{|n_R - R + 0.5|}{\sigma_R} \quad Z_{tm} = \frac{|n_R - R - 0.5|}{\sigma_R} \quad (31)$$

Here, the sub-indices tf and tm stand for too few and too many runs, respectively. The corrections +0.5 and –0.5 are required for correcting for the approximation of a binomial distribution by a normal one. By setting the probability of false alarm as α , the critical region is $Z \geq Q(\alpha/2) = 1/\sqrt{2\pi} \int_{\alpha/2}^{\infty} \exp(-t^2/2) dt$. For 95% confidence ($\alpha = 0.05$), the hypothesis test (fitting acceptability) requires that the critical value for the estimated normal deviate be $Z_{cr} = 0.976$. In the analyzed cases of this work, the number of experimental data was not higher than 15, such that the runs tests will be made on the basis of the stringent value Z_{tf} (i.e., too few runs).

Conflict of Interest

The authors declare no conflict of interest.

Keywords

amylolysis, mathematical model, Michaelis–Menten kinetics, rapidly and slowly digestible starch

Received: July 1, 2019
Revised: October 28, 2019
Published online:

- [1] E. Giovannucci, *Am. J. Clin. Nutr.* **2007**, *86*, 836S.
- [2] I. Goñi, A. G. Alonso, F. S. Calixto, *Nutr. Res.* **1997**, *17*, 427.
- [3] P. J. Butterworth, F. J. Warren, T. Grassby, H. Patel, P. R. Ellis, *Carbohydr. Polym.* **2012**, *87*, 2189.
- [4] H. Patel, R. Day, P. J. Butterworth, P. R. Ellis, *Carbohydr. Polym.* **2014**, *113*, 182.
- [5] C. Åkerberg, G. Zacchi, N. Torto, L. Gorton, *J. Chem. Tech. Biotech.* **2000**, *75*, 306.
- [6] M. E. Amato, G. Ansanelli, S. Fisichella, R. Lamanna, G. Scarlata, A. P. Sobolev, A. Segre, *J. Agr. Food Chem.* **2004**, *52*, 823.
- [7] A. C. Dona, G. Pages, R. G. Gilbert, M. Gaborieau, P. W. Kuchel, *Biomacromolecules* **2009**, *10*, 638.
- [8] A. C. Dona, G. Pages, R. G. Gilbert, P. W. Kuchel, *Carbohydr. Polym.* **2010**, *80*, 599.
- [9] H. N. Englyst, S. M. Kingman, J. H. Cummings, *Eur. J. Clinical Nutr.* **1992**, *46*, S33.
- [10] G. A. Hill, D. G. Macdonald, X. Lang, *Biotechnol. Lett.* **1997**, *19*, 1139.
- [11] D. K. Apar, B. Özbek, *Process Biochem.* **2004**, *39*, 1877.
- [12] K. Okamoto, B. T. Eger, T. Nishino, S. Kondo, E. F. Pai, T. Nishino, *J. Biol. Chem.* **2003**, *278*, 1848.
- [13] I. Buch, T. Giorgino, G. De Fabritiis, *Proc. Nat. Acad. Sci.* **2011**, *108*, 10184.
- [14] C. S. Berry, *J. Cereal Sci.* **1986**, *4*, 301.
- [15] I. Goñi, L. Garcia-Diaz, E. Mañas, F. Saura-Calixto, *Food Chem.* **1996**, *56*, 445.
- [16] B. Zhang, S. Dhital, B. M. Flanagan, M. J. Gidley, *J. Agri. Food Chem.* **2014**, *62*, 760.
- [17] M. J. Van Der Maarel, B. Van der Veen, J. C. Uitdehaag, H. Leemhuis, L. Dijkhuizen, *J. Biotech.* **2002**, *94*, 137.
- [18] G. L. Miller, *Anal. Chem.* **1959**, *31*, 426.
- [19] J. W. Tukey, *Biometrics*, **1949**, *5*, 99.
- [20] M. Straume, M. L. Johnson, in *Methods in Enzymology*, Vol. 210, Academic Press, San Diego, CA **1992**, pp. 87–105.
- [21] M. A. J. S. Van Boekel, *Food Res. Int.* **1999**, *32*, 261.